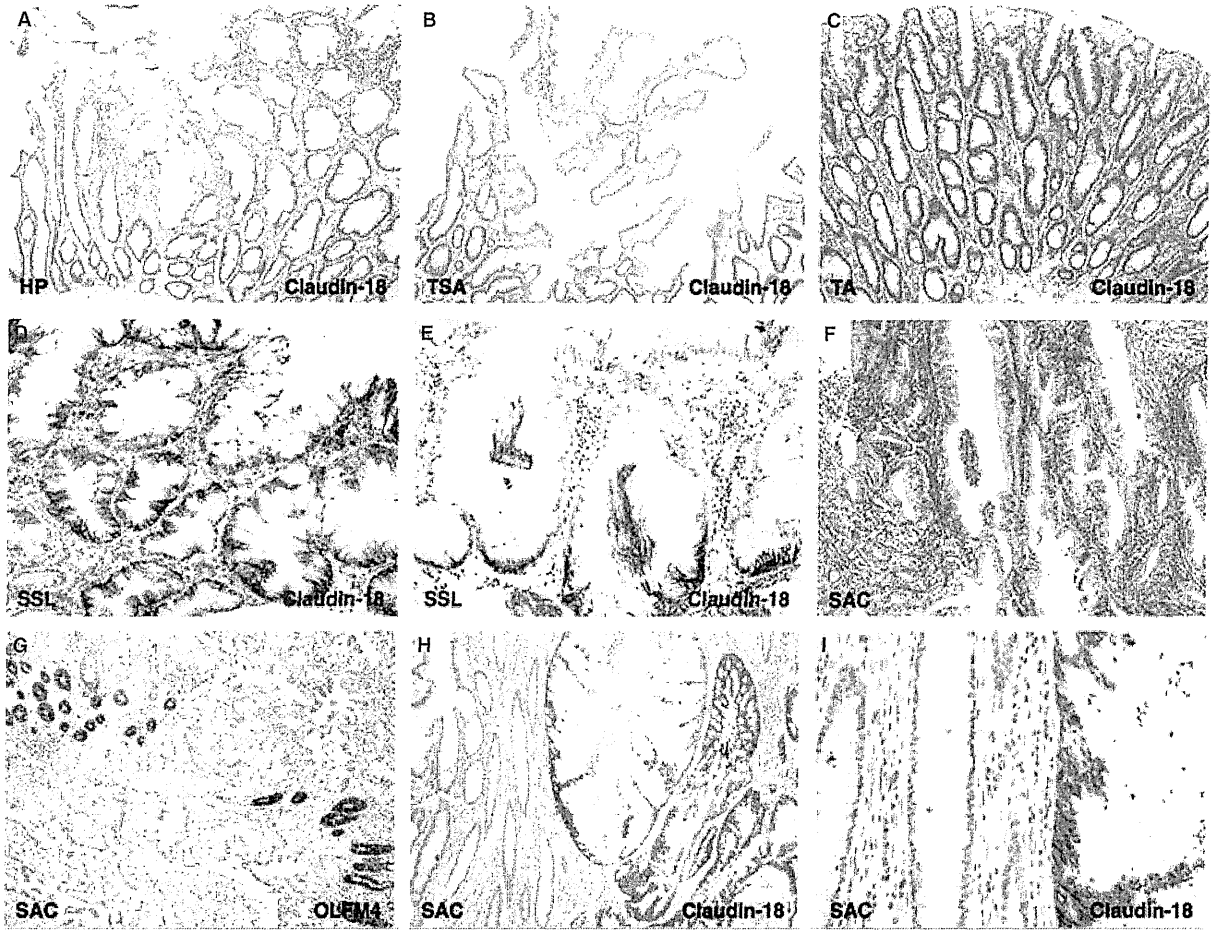

Figure 2. Immunohistochemical staining for claudin-18 or olfactomedin 4 (OLFM4) in various colorectal polyps and serrated adenocarcinoma (SAC). A–E, Some sessile serrated lesions (SSL) showed membranous staining for claudin-18, compared with other colorectal polyps. F, H&E staining of SAC. G–I, Loss of expression of OLFM4 and/or increased expression of claudin-18 was observed in SAC.

polyps expressed claudin-18, whereas corresponding non-neoplastic colorectal mucosa did not express claudin-18. Claudin-18-positive SAC cases showed more advanced N grade ($P = 0.022$) and stage ($P = 0.022$) than did claudin-18-negative SAC cases, but claudin-18 staining did not correlate with any clinicopathological parameters in the non-SAC cases.

Discussion

There is growing evidence that a subset of serrated colorectal polyps may serve as precursor lesions for CRC resulting from the serrated pathway.[27,28] Of these polyps, SSL bear a closer histological resemblance to the traditional HP than to TSA or CA, which are identified easily on H&E-stained slides. Morphological criteria have been proposed to distinguish SSL from traditional HP.[4,5] These criteria take into account the location and size of the polyp and the architectural and cytological features of the crypt. The application of morphological criteria leads inevitably to intraobserver and interobserver variability, and specimen orientation and cautery artefacts can also interfere with interpretation. A biomarker that delineates conventional benign serrated polyps from SSL objectively and reproducibly would help practising pathologists in assessing equivocal cases. In the present study, we demonstrated clearly that olfactomedin 4 and claudin-18 are useful immunohistochemical markers of SSL.

Various serrated lesions have characteristic abnormalities of the proliferative zone and resultant architectural changes.[22] In SSL, as-yet unknown factors lead to alterations in the location of the proliferative

Table 2. Olfactomedin 4 expression and clinicopathological parameters in 36 colorectal serrated adenocarcinomas and 218 non-serrated adenocarcinomas

	Serrated (n = 36)			Non-serrated (n = 218)		
	Positive	Negative	P value	Positive	Negative	P value
Total	3 (8%)	33	–	75 (34%)	143	–
Age (years)						
≤65	0	13	NS	39 (34%)	76	NS
>65	3 (13%)	20	–	36 (35%)	67	–
Sex						
Male	3 (21%)	11	NS	41 (34%)	81	NS
Female	0	22	–	34 (35%)	62	–
Tumour location						
Right/transverse	0	15	NS	18 (32%)	38	NS
Left/sigmoid/rectum	3 (14%)	18	–	57 (35%)	105	–
T grade						
Tis/T1/T2	1 (20%)	4	NS	30 (42%)	42	NS
T3/T4	2 (6%)	29	–	45 (31%)	101	–
N grade						
N0	2 (13%)	14	NS	52 (40%)	78	0.041
N1/N2	1 (5%)	19	–	23 (26%)	65	–
M grade						
M0	2 (6%)	31	NS	67 (35%)	122	NS
M1	1 (33%)	2	–	8 (28%)	21	–
Stage						
0/I/II	2 (13%)	14	NS	51 (40%)	75	0.031
III/IV	1 (5%)	19	–	24 (26%)	68	–
Histological type						
Well/moderately	3 (10%)	27	NS	73 (35%)	136	NS
Poorly/mucinous	0	6	–	2 (22%)	7	–

NS, Not significant.

zone away from its usual location in the base of the crypts, resulting in maturation which may develop towards the base of the crypts and lead to distortion of the crypt architecture, commonly with dilated or L-, inverted T- or anchor-shaped crypts with mature cells where the proliferative zone is normally located.[8] In this study, the proliferation marker Ki67 showed variable staining in colorectal serrated polyps. However, Ki67 does not appear helpful in distinguishing SSL from HP in pathology practice, as reported previously.[29] There were roughly similar distributions of olfactomedin 4 and Ki67 expression in HP, TSA and CA. This result appeared to be convincing when the localization and role of olfactomedin 4 in proliferation and cell cycle progression was considered.[17] However, positivity for olfactomedin 4 in SSL was significantly lower than that for Ki67. There are, to our knowledge, no previous reports of the reduction or loss of olfactomedin 4 in SSL. However, reduced expression of olfactomedin 4 was reported to be regulated at the transcriptional or post-transcriptional level rather than at the genomic level in CRC.[30] The most

Table 3. Claudin-18 expression and clinicopathological parameters in 36 colorectal serrated adenocarcinomas and 218 non-serrated adenocarcinomas

	Serrated (n = 36)			Non-serrated (n = 218)		
	Positive	Negative	P value	Positive	Negative	P value
Total	10 (28%)	26	–	11 (5%)	207	–
Age (years)						
≤65	3 (23%)	10	NS	5 (4%)	110	NS
>65	7 (30%)	16	–	6 (6%)	97	–
Sex						
Male	6 (43%)	8	NS	5 (4%)	117	NS
Female	4 (18%)	18	–	6 (6%)	90	–
Tumour location						
Right/transverse	4 (27%)	11	NS	4 (7%)	52	NS
Left/sigmoid/rectum	6 (29%)	15	–	7 (4%)	155	–
T grade						
Tis/T1/T2	0	5	NS	4 (6%)	68	NS
T3/T4	10 (32%)	21	–	7 (5%)	139	–
N grade						
N0	1 (6%)	15	0.022	6 (5%)	124	NS
N1/N2	9 (45%)	11	–	5 (6%)	83	–
M grade						
M0	8 (32%)	25	NS	8 (4%)	181	NS
M1	2 (67%)	1	–	3 (10%)	26	–
Stage						
0/I/II	1 (6%)	15	0.022	5 (4%)	121	NS
III/IV	9 (45%)	11	–	6 (7%)	86	–
Histological type						
Well/moderately	8 (27%)	22	NS	11 (5%)	198	NS
Poorly/mucinous	2 (33%)	4	–	0	9	–

NS, Not significant.

common CRCs arising via the serrated pathway are prone to methylation of the CpG island promoter regions, resulting in epigenetic silencing of a number of genes. It is presumed that the specific genes silenced may be random events. The most well-characterized epigenetic silencing in these lesions is that of the *hMLH1* gene, which is silenced in sporadic microsatellite instability carcinomas. Aberrant hypermethylation of bone morphogenic protein 3 was also observed frequently in colorectal tumours progressing via the serrated pathways.[31] On the basis of the results of the present study, methylation of olfactomedin 4 might occur in SSL. In the present study, expression of olfactomedin 4 in SAC was also significantly lower than that in non-SAC. Furthermore, right-sided SAC did not express olfactomedin 4.

Claudin family members are crucial components of tight junctions and show highly tissue-specific patterns.[32] We have reported previously that retained claudin-18, which is expressed in normal stomach, correlates with a survival benefit in gastric cancer.[26] Conversely, ectopic expression of claudin-18, which is

not expressed in normal colon, correlates with poor survival in CRC.[20] However, little is known about the biological significance of claudin-18 in colorectal serrated polyps. In this study, we showed that claudin-18 was expressed in 44% of SSL, 12% of TSA and 28% of SAC cases. Both SSL and TSA have been reported to display the gastric mucin phenotype.[33] CRC with gastric phenotype show frequent lymphatic permeation and lymph node metastasis,[34] and a close association with specific genetic subtypes such as microsatellite instability (MSI). *CDX2* was also reported to be mutated in CRC with MSI-H.[3] We have reported previously that the positive expression of claudin-18 correlated significantly with the positive expression of MUC5AC and the negative expression of CDX2.[20] SOX2 is an HMG-box transcription factor expressed in gastric mucosa but not in intestine. Park *et al.*[35] reported that aberrant expression of SOX2 up-regulated MUC5AC in CRC. In addition, Tsukamoto *et al.*[36] reported that the immunohistochemical expression patterns of SOX2 and CDX2 were related inversely in the human stomach. In the present study, non-neoplastic colorectal mucosa and colorectal polyps other than SSL and TSA did not express claudin-18.

In summary, we have performed an immunohistochemical analysis of olfactomedin 4 and claudin-18 in serrated neoplasia of the colorectum. A characteristic expression pattern of these molecules was observed in serrated polyps, especially in SSL. Reduced expression of olfactomedin 4 and ectopic expression of claudin-18 might be associated with the serrated pathway of colorectal carcinogenesis, and these markers may be useful in the differential diagnosis of serrated polyps.

References

1. Snover DC. Serrated polyps of the large intestine. *Semin. Diagn. Pathol.* 2005; 22; 301–308.
2. Rashid A, Houlihan PS, Booker S, Petersen GM, Giardiello FM, Hamilton SR. Phenotypic and molecular characteristics of hyperplastic polyposis. *Gastroenterology* 2000; 119; 323–332.
3. Jass JR. Classification of colorectal cancer based on correlation of clinical, morphological and molecular features. *Histopathology* 2007; 50; 113–130.
4. Torlakovic E, Skovlund E, Snover DC, Torlakovic G, Nesland JM. Morphologic reappraisal of serrated colorectal polyps. *Am. J. Surg. Pathol.* 2003; 27; 65–81.
5. Goldstein NS, Bhanot P, Odish E, Hunter S. Hyperplastic-like colon polyps that preceded microsatellite-unstable adenocarcinomas. *Am. J. Clin. Pathol.* 2003; 119; 778–796.
6. Farris AB, Misdraji J, Srivastava A *et al.* Sessile serrated adenoma: challenging discrimination from other serrated colonic polyps. *Am. J. Surg. Pathol.* 2008; 32; 30–35.
7. Ngo NT, Tan E, Tekkis P, Peston D, Cohen P. Differential expression of p53 and p504s in hyperplastic polyp, sessile serrated adenoma and traditional serrated adenoma. *Int. J. Colorect. Dis.* 2010; 25; 1193–1200.
8. Torlakovic EE, Gomez JD, Driman DK *et al.* Sessile serrated adenoma (SSA) vs. traditional serrated adenoma (TSA). *Am. J. Surg. Pathol.* 2008; 32; 21–29.
9. Owens SR, Chiosea SI, Kuan SF. Selective expression of gastric mucin MUC6 in colonic sessile serrated adenoma but not in hyperplastic polyp aids in morphological diagnosis of serrated polyps. *Mod. Pathol.* 2008; 21; 660–669.
10. Gibson JA, Hahn HP, Shahsafaei A, Odze RD. MUC expression in hyperplastic and serrated colonic polyps: lack of specificity of MUC6. *Am. J. Surg. Pathol.* 2011; 35; 742–749.
11. Schmitz KJ, Hey S, Schinwald A *et al.* Differential expression of microRNA 181b and microRNA 21 in hyperplastic polyps and sessile serrated adenomas of the colon. *Virchows Arch.* 2009; 455; 49–54.
12. Tuppurainen K, Mäkinen JM, Junttila O *et al.* Morphology and microsatellite instability in sporadic serrated and non-serrated colorectal cancer. *J. Pathol.* 2005; 207; 285–294.
13. Noffsinger AE. Serrated polyps and colorectal cancer: new pathway to malignancy. *Annu. Rev. Pathol.* 2009; 4; 343–364.
14. Yasui W, Oue N, Sentani K, Sakamoto N, Motoshita J. Transcriptome dissection of gastric cancer: identification of novel diagnostic and therapeutic targets from pathology specimens. *Pathol. Int.* 2009; 59; 121–136.
15. Zhang X, Huang Q, Yang Z, Li Y, Li CY. GW112, a novel antiapoptotic protein that promotes tumor growth. *Cancer Res.* 2004; 64; 2474–2481.
16. Seko N, Oue N, Noguchi T *et al.* Olfactomedin 4 (GW112, hGC-1) is an independent prognostic marker for survival in patients with colorectal cancer. *Exp. Ther. Med.* 2010; 1; 73–78.
17. van der Flier LG, Haegebarth A, Stange DE, van de Wetering M, Clevers H. OLFM4 is a robust marker for stem cells in human intestine and marks a subset of colorectal cancer cells. *Gastroenterology* 2009; 137; 15–17.
18. Tsukita S, Furuse M, Itoh M. Multifunctional strands in tight junctions. *Nat. Rev. Mol. Cell Biol.* 2001; 2; 285–293.
19. Zwiers A, Fuss IJ, Leijen S, Mulder CJ, Kraal G, Bouma G. Increased expression of the tight junction molecule claudin-18 A1 in both experimental colitis and ulcerative colitis. *Inflamm. Bowel Dis.* 2008; 14; 1652–1659.
20. Matsuda M, Sentani K, Noguchi T *et al.* Immunohistochemical analysis of colorectal cancer with gastric phenotype: claudin-18 is associated with poor prognosis. *Pathol. Int.* 2010; 60; 673–680.
21. Sentani K, Oue N, Tashiro T *et al.* Immunohistochemical staining of Reg IV and claudin-18 is useful in the diagnosis of gastrointestinal signet ring cell carcinoma. *Am. J. Surg. Pathol.* 2008; 32; 1182–1189.
22. Snover DC. Update on the serrated pathway to colorectal carcinoma. *Hum. Pathol.* 2011; 42; 1–10.
23. García-Solano J, Pérez-Guillermo M, Conesa-Zamora P *et al.* Clinicopathologic study of 85 colorectal serrated adenocarcinomas: further insights into the full recognition of a new subset of colorectal carcinoma. *Hum. Pathol.* 2010; 41; 1359–1368.
24. Hamilton SR, Aaltonen LA (eds). *World Health Organization classification of tumours. Pathology and genetics of tumours of the digestive system.* Lyon: IARC Press, 2000; 104–111.
25. Oue N, Sentani K, Noguchi T *et al.* Serum olfactomedin 4 (GW112, hGC-1) in combination with Reg IV is a highly sensi-

tive biomarker for gastric cancer patients. *Int. J. Cancer* 2009; **125**; 2383–2392.
26. Sanada Y, Oue N, Mitani Y, Yoshida K, Nakayama H, Yasui W. Down-regulation of the claudin-18 gene, identified through serial analysis of gene expression data analysis, in gastric cancer with an intestinal phenotype. *J. Pathol.* 2006; **208**; 633–642.
27. O'Brien MJ, Yang S, Clebanoff JL *et al.* Hyperplastic (serrated) polyps of the colorectum: relationship of CpG island methylator phenotype and K-ras mutation to location and histologic subtype. *Am. J. Surg. Pathol.* 2004; **28**; 423–434.
28. Huang CS, O'Brien M J, Yang S, Farraye FA. Hyperplastic polyps, serrated adenomas, and the serrated polyp neoplasia pathway. *Am. J. Gastroenterol.* 2004; **99**; 2242–2255.
29. Gray D, Obermann EC, Evans M, Hartmann A, Cooper K, Blaszyk H. MIB-1 and MCM-2 immunohistochemical analysis does not aid in identification of serrated colorectal polyps with abnormal proliferation. *Am. J. Clin. Pathol.* 2006; **125**; 407–412.
30. Liu W, Liu Y, Zhu J, Wright E, Ding I, Rodgers GP. Reduced hGC-1 protein expression is associated with malignant progression of colon carcinoma. *Clin. Cancer Res.* 2008; **14**; 1041–1049.
31. Loh K, Chia JA, Greco S *et al.* Bone morphogenic protein 3 inactivation is an early and frequent event in colorectal cancer development. *Genes Chromosom. Cancer* 2008; **47**; 449–460.
32. Hewitt KJ, Agarwal R, Morin PJ. The claudin gene family: expression in normal and neoplastic tissues. *BMC Cancer* 2006; **6**; 186.
33. Fujita K, Hirahashi M, Yamamoto H *et al.* Mucin core protein expression in serrated polyps of the large intestine. *Virchows Arch.* 2010; **457**; 443–449.
34. Yao T, Tsutsumi S, Akaiwa Y *et al.* Phenotypic expression of colorectal adenocarcinomas with reference to tumor development and biological behavior. *Jpn. J. Cancer Res.* 2001; **92**; 755–761.
35. Park ET, Gum JR, Kakar S, Kwon SW, Deng G, Kim YS. Aberrant expression of SOX2 upregulates MUC5AC gastric foveolar mucin in mucinous cancers of the colorectum and related lesions. *Int. J. Cancer* 2008; **122**; 1253–1260.
36. Tsukamoto T, Inada K, Tanaka H *et al.* Down-regulation of a gastric transcription factor, Sox2, and ectopic expression of intestinal homeobox genes, Cdx1 and Cdx2: inverse correlation during progression from gastric/intestinal-mixed to complete intestinal metaplasia. *J. Cancer Res. Clin. Oncol.* 2004; **130**; 135–145.

European Journal of Radiology 82 (2013) 169–176

Contents lists available at SciVerse ScienceDirect

European Journal of Radiology

journal homepage: www.elsevier.com/locate/ejrad

Evaluation of the efficacy of the guideline on reading CT images of malignant pleural mesothelioma with reference CT films for improving the proficiency of radiologists

Huashi Zhou[a,1], Taro Tamura[a,2], Yukinori Kusaka[a,*], Narufumi Suganuma[b,3], Ponglada Subhannachart[c,4], Chomphunut Vijitsanguan[c,4], Weeraya Noisiri[c,4], Kurt G. Hering[d,5], Masanori Akira[e,6], Harumi Itoh[a,f,7], Hiroaki Arakawa[g,8], Yuichi Ishikawa[h,9], Shinji Kumagai[i,10], Norio Kurumatani[j,11]

[a] Department of Environmental Health, School of Medicine University of Fukui, 23-3 Shimoaitsuki, Matsuoka, Eihezi-cho, Fukui Prefecture, 910-1193, Japan
[b] Department of Environmental Medicine, Kochi University School of Medicine, Japan
[c] Central Chest Disease Institute of Thailand, 39 Moo 9, Tiwanon Road, Muang Nonthaburi, 11000, Thailand
[d] Department of Diagnostic Radiology, Radiooncology and Nuclear Medicine, Radiological Clinic, Miner's Hospital, Radiologische Klinik, Lansppaschaftskranhaus Dortmund, Wieckesweg 27, 44309, Dortmund, Germany
[e] Department of Radiology, National Hospital Organization Kinki-Chuo Chest Medical Center, 1180 Nagasone-cho, Kita-ku, Sakai, Osaka, 591-8555, Japan
[f] Department of Radiology, School of Medicine, University of Fukui, 23-3 Shimoaitsuki Matsuoka, Eiheizi-cho, Fukui Prefecture, 910-1193, Japan
[g] Department of Radiology, Dokkyo University School of Medicine, 880 Oaza-Kitakobayashi, Mibu-cho, Shimotsuga-gun, Tochigi, 321-0207, Japan
[h] Department of Pathology, Cancer Institute, 1-37-1 Kami-ikebukuro, Toshima-ku, Tokyo, 170-8455, Japan
[i] Department of Environmental Management, School of Health Sciences, University of Occupational and Environmental Health, University of Occupational and Environmental Health, 1-1, Iseigaoka, Yahata-nishi-ku, Fukuoka, Kitakyushu, 807-8555, Japan
[j] Department of Community Health and Epidemiology, Nara Medical University School of Medicine, 840 Shijo-cho Kashihara, Nara, 634-8521, Japan

ARTICLE INFO

Article history:
Received 2 March 2012
Received in revised form 20 May 2012
Accepted 21 May 2012

Keywords:
Computed tomography
Malignant pleural mesothelioma
Guideline
Sensitivity
Specificity
Agreement

ABSTRACT

Purpose: To assess the efficacy of the developed guideline on reading CT images of malignant pleural mesothelioma for improving radiologists' reading proficiency.
Materials and Methods: Three radiologists independently read the CT films of 22 cases including definite mesothelioma and non-mesothelioma cases at two times before and after studying the malignant pleural mesothelioma CT Guideline. The sensitivity and specificity for mesothelioma were calculated and compared between the 1st and 2nd trials. The kappa statistics was examined for agreement with experts for mesothelioma probability and for mesothelioma features recorded by three radiologists.
Results: After studying the mesothelioma CT Guideline, the sensitivity for mesothelioma shown by the three radiologists at the 2nd trial was 100%, 100% and 80%, which were higher than 80%, 85% and 60% at the 1st trial, respectively. The average kappa for agreement between radiologists and experts on dichotomized mesothelioma probability were 0.69 (good) at the 2nd trial vs. 0.38 (fair) at the 1st trial. The average kappa for the agreement with experts for each of 7 features by three radiologists were 0.52–0.80 at the 2nd trial, which were significantly higher than 0.34–0.58 at the 1st trial (Wilcoxon Signed Rank Test: $P<0.01$), and as to five features "unilateral pleural effusion", "nodular pleural thickening", "tumoral encasement of lung", "mediastinal pleural thickening", and "diminished lung", they achieved good agreement with average kappa of 0.61–0.80.
Conclusion: The developed mesothelioma CT Guideline was suggested to have substantial effect in improving the radiologists' proficiency for reading CT images of mesothelioma, and may contribute to accurate diagnosis of mesothelioma.

* Corresponding author. Tel.: +81 776 61 8335; fax: +81 776 61 8107.
E-mail addresses: zhouhua@u-fukui.ac.jp (H. Zhou), tarou@u-fukui.ac.jp (T. Tamura), kusakayk@gmail.com (Y. Kusaka), nsuganuma@kochi-u.ac.jp (N. Suganuma), pongladas@gmail.com (P. Subhannachart), Chompoo_vj@yahoo.com (C. Vijitsanguan), weeraya_tat@yahoo.com (W. Noisiri), k.g.hering@t-online.de (K.G. Hering), akira@kch.hosp.go.jp (M. Akira), hitoh@fmsrsa.fukui-med.ac.jp (H. Itoh), arakawa@dokkyomed.ac.jp (H. Arakawa), ishikawa@jfcr.or.jp (Y. Ishikawa), shkumagai@health.uoeh-u.ac.jp (S. Kumagai), knorio@naramed-u.ac.jp (N. Kurumatani).
[1] Tel.: +81 776 61 8338; fax: +81 776 61 8107.
[2] Tel.: +81 776 61 8335; fax: +81 776 61 8107.
[3] Tel.: +81 88 880 2407; fax: +81 88 880 2407.
[4] Tel.: +66 2 5803423x7505; fax: +66 2 5806992.
[5] Tel.: +49 0 231 9221280; fax: +49 0 231 9221648.
[6] Tel.: +81 722 52 3021; fax: +81 722 51 1372.
[7] Tel.: +81 776 61 8368; fax: +81 776 61 8137.
[8] Tel.: +81 282 87 2171; fax: +81 282 86 4940.
[9] Tel.: +81 3 3570 0448; fax: +81 3 3570 0558.
[10] Tel.: +81 93 691 7282; fax: +81 93 691 2694.
[11] Tel.: +81 744 298841; fax: +81 744 290673.

0720-048X/$ – see front matter © 2012 Elsevier Ireland Ltd. All rights reserved.
http://dx.doi.org/10.1016/j.ejrad.2012.05.022

1. Introduction

The *International Classification of HRCT for Occupational and Environmental Respiratory Diseases* (ICOERD) was developed and used for occupational diseases screening, epidemiology study, and clinical study for respiratory diseases caused by occupational and environmental factors [1]. In order to supply ICOERD, we have developed the *Guideline on Reading CT Films of Malignant Pleural Mesothelioma* (MPM-CT Guideline) and selected MPM reference CT films [2]. The MPM-CT Guideline provides the terminology of MPM CT features and the MPM probability, the judgment for MPM in terms of involvement distribution and severity, as well as a method to record the CT finding of MPM on the CT reading sheet. The purpose of the current study was to investigate the efficacy of the developed MPM-CT Guideline with the MPM reference CT films for improving the proficiency of the inexperienced radiologists in reading CT images of MPM.

2. Materials and methods

2.1. Subject CT films

CT films of fifty seven cases including MPM, lung cancer, other malignancies, and benign pleural plaque were collected from the citizens living in the neighborhood of the Kubota factory, a large asbestos cement pipe factory in Amagasaki City, Hyogo Prefecture, Japan. Their MPM was caused by environmental exposure to asbestos (mainly crocidolite) air pollution from the Kubota asbestos factory [3].

Out of the 57 cases, 22 cases including 20 definite MPM cases and 2 pleural plaque cases were subjected to study. The MPM cases were clinically diagnosed as MPM at local hospitals and both pathologically and immunohistochemically confirmed [4,5]. Among the 20 cases of MPM, 7 cases were female, and 13 cases were male. The two cases of pleural plaque were male.

Among the 20 MPM cases, the diffuse type of MPM accounted for 18 (90%), and the localized type for the other 2 cases (10%). The numbers of the cases with MPM CT features among 20 MPM cases by MPM probability are shown in Table 1. The CT images of several representative MPM cases among the 20 MPM cases are shown as Figs. 1–5.

2.2. The MPM reference CT films

The MPM reference CT films and CT subject images were used by radiologists only at the 2nd reading trial for comparison of the subjects' CT findings with MPM reference films. The ten typical MPM features on the reference CT films included "unilateral pleural effusion" ("ue"), "nodular pleural thickening" ("nt"), "interlobar fissure thickening" ("it"), "mediastinal pleural thickening" ("mt"), "tumoral encasement of lung" ("te"), "calcified plaque engulfment" ("pe"), "invasion" (iv"), "diminished lung" ("dl"), "contracted hemithorax" ("ch") and "pleural mass" ("pm"). Each MPM feature was indicated by an arrow on the reference CT digital images and hard-copied CT reference films. The CT images of typical MPM features are shown as in Fig. 1 through Fig. 9 in a parallel publication [2].

2.3. CT reading trials of 22 cases by three radiologists

Three radiologists participated in independent reading of CT films. All of the radiologists had good proficiency and rich experience in reading CT for pneumoconioses. However, they had not seen many MPM cases previously. Before achieving the 1st and 2nd reading trials, they were blinded to the information of the patients' asbestos exposure history, and the clinical and histological diagnosis for any cases.

At the 1st CT reading trial, the three radiologists were requested to read the monograph of ICOERD and the ICOERD CT reference films, but not to read the MPM-CT Guideline nor the MPM reference CT films, then they read the 22 subject CT films independently. The CT findings associated with asbestosis were recorded according to ICOERD guideline; the MPM features and the MPM probability grade for each case were recorded into the reading sheet according to their experiences.

The interval between the 1st and the 2nd CT reading trials by the three radiologists was at least three months. At the 2nd trial, before reading the subject CT films, the three radiologists read the ICOERD guideline with the ICOERD CT reference films again. They also independently studied the MPM-CT Guideline with the MPM reference CT films, and then independently read the 22 subject CT films. They made use of the ICOERD CT reference films and the MPM reference CT films to record the CT findings for pneumoconiosis, the MPM findings, and the MPM probability grade in the CT reading sheets.

2.4. Statistical analysis

According to the definition for the MPM probability in the MPM-CT Guideline [2], Grade 1 was negative for MPM, no abnormal findings on CT, or the abnormal findings of other diseases; Grade 2 was low probability of MPM; Grade 3 was moderate probability of MPM; Grade 4 was high probability of MPM. Sensitivity for MPM was the proportion of cases for which MPM probability Grade $\geq$2 recorded by radiologists for each among the 20 MPM cases. Specificity for MPM was the proportion of cases for which MPM probability Grade = 1 was recorded by individual radiologists among the 2 non-MPM cases, shown as Table A in Supplementary Appendix. The sensitivity and specificity for MPM by the three radiologists were calculated and compared between the 1st and the 2nd reading trials.

The weighted kappa for the agreement of the three individual radiologists with the consensus by the four experts (K.G.H., M.A., H. A., H. I.) on the 4-point scale MPM probability was calculated using R-software version 2.14.1 (http://www.r-project.org/), as shown in Table B in Supplementary Appendix. The kappa for the agreement on dichotomized MPM probability was calculated by stratifying the cases with MPM probability Grade 2, 3, 4 into one group, and the cases with MPM probability Grade = 1 into the other group, as shown in Table C in the Supplementary Appendix. The observed agreement on dichotomized MPM probability between radiologist and experts was also calculated. The calculation of kappa for the agreement on MPM CT feature between radiologist and experts is shown as Table D in the Supplementary Appendix. A kappa value <0.20 was considered as poor agreement, 0.21–0.40 was as fair agreement, 0.41–0.60 was as moderate agreement, 0.61–0.80 was as good agreement, and 0.81–1.00 was as excellent agreement [6]. The kappa values for the 7 MPM CT features by the three radiologists between the 1st trial and 2nd trial were compared by 2-Related-Samples Nonparametric Test (Wilcoxon Signed Rank Test).

3. Results

3.1. The MPM probability and the 7 MPM CT features among the 20 MPM cases

The MPM probability and the 7 MPM CT features (7-MPM-CT features) agreed by the four experienced experts for the 20 subject cases of MPM are shown as Table 1.

Table 1
The number of cases with the 7-MPM-CT features among the 20 MPM cases according to MPM probability.

Cases with MPM probability	The number of cases with the MPM feature						
	ue	nt	it	mt	te	iv	dl
Grade=1 (n=0)	0	0	0	0	0	0	0
Grade=2 (n=3)	0	1	0	0	0	2	0
Grade=3 (n=7)	5	2	4	7	0	1	4
Grade=4 (n=10)	8	10	7	10	5	6	10
Total (n=20)	13(65%)	13(65%)	11(55%)	17(85%)	5(25%)	9(45%)	14(70%)

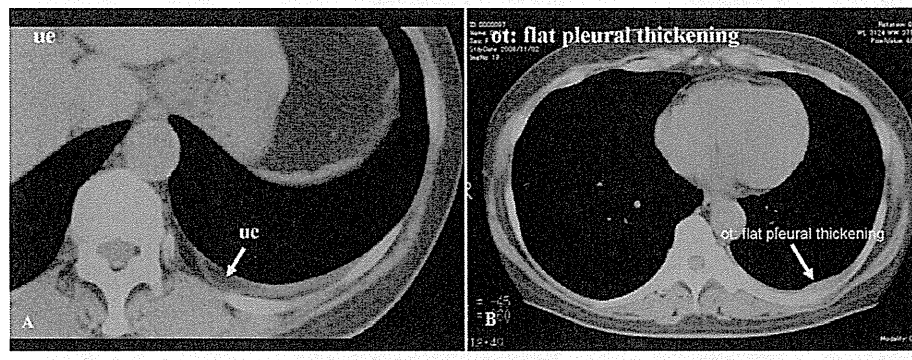

Fig. 1. A 52-year-old women with diffuse epithelioid MPM. CT scans show slight unilateral pleural effusion (A) and flat pleural thickening in the left hemithorax (B). According to the CT appearance, the MPM probability was agreed as low probability Grade 2 at mild severity by experts.

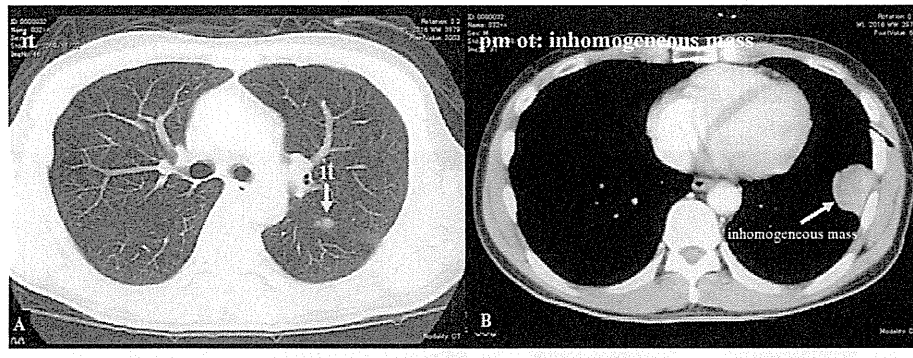

Fig. 2. A 49-year-old man with biphasic MPM. CT scans show interlobar fissure pleural thickening ("it") at the left lung (A), and the left-side pleural mass with involvement of chest wall (B). According the CT appearance, the MPM probability was agreed by experts as low probability Grade 2. The differential diagnosis for this case is mainly sarcoma.

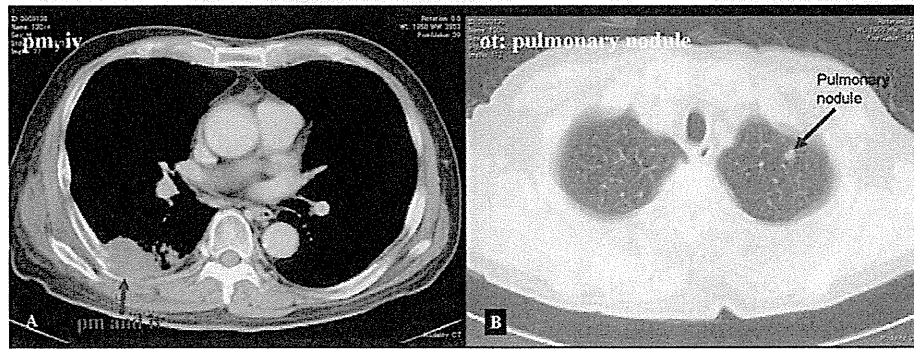

Fig. 3. A 68-year-old man with localized sarcomatoid MPM. CT scan demonstrates a right-sided pleural mass invasion ("iv") to the chest wall destroying rib structure (arrow) (A). There is a pulmonary nodule on the left lung (B). This case was agreed as MPM of moderate probability Grade 3 at advanced severity. The different diagnosis is firstly sarcoma and secondly possible metastasis from other cancer.

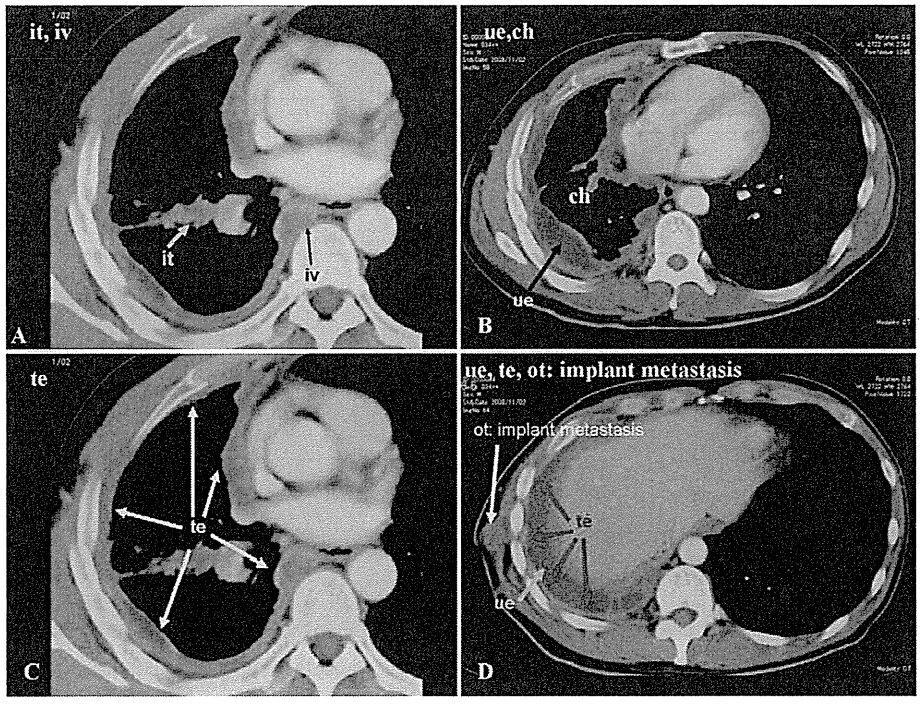

Fig. 4. A 45-year-old man with diffuse epithelioid MPM. CT scan shows interlobar fissure pleural thickening (A), invasion to the tissue near to the vertebral column ("iv") (black arrow) (A). There is unilateral pleural effusion ("ue") (black arrow) on the right hemithorax, leading to the contracted hemithorax ("ch") (B). Tumoral encasement of lung ("te") involvement on the right hemithorax (C, D) and an implant metastasis lesion are observed on the chest wall of right lung (D). According the CT appearance, MPM probability was agreed by experts as high probability Grade 4 at advanced severity. This is a typical MPM case.

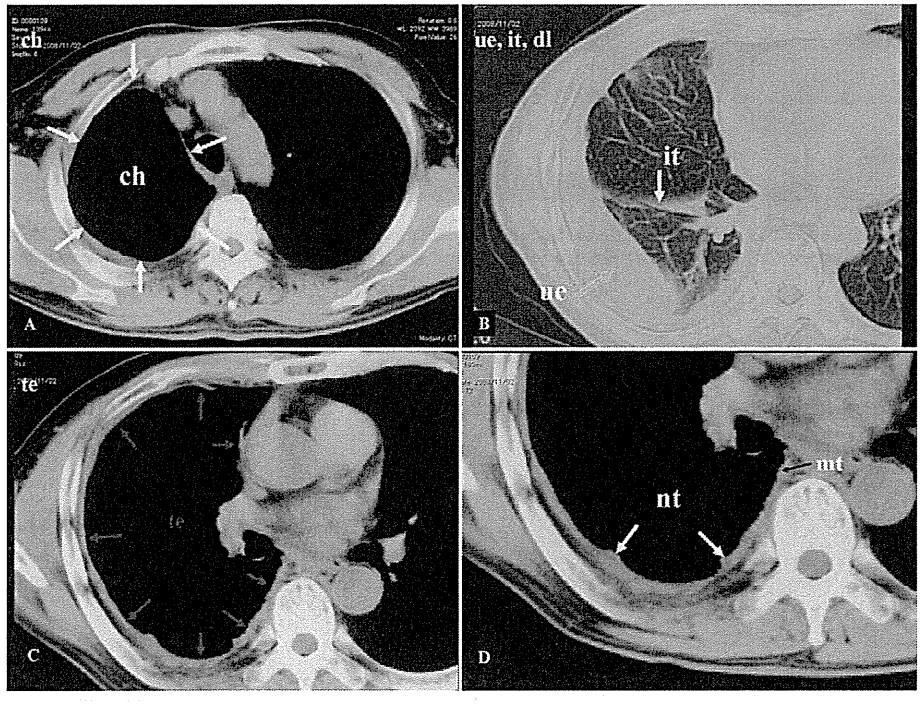

Fig. 5. A 58 year-old man with diffuse desmoplastic MPM. CT scan shows contracted hemithorax ("ch") leading to the right hemithorax volume loss (A). There is interlobar fissure pleural thickening ("it"), together with unilateral pleural thickening ("ue"), causing the lung volume diminished ("dl") (B). The involvement of tumoral encasement of lung ("te") (C), nodular pleural thickening ("nt") and mediastinal pleural thickening ("mt") (black arrow) on the right hemithorax are observed (D). MPM probability was agreed by experts as high MPM probability Grade 4 at advanced severity. This is a typical MPM case.

Table 2
Agreement on dichotomized MPM probability with 4 experts' consensus and sensitivity and specificity for MPM by three radiologists at the two trials.

Reader	Reading trial	Agreement with experts on dichotomized MPM probability	Sensitivity for MPM	Specificity for MPM
Radiologist 1	1st	18/22 (81.82%)	16/20 (80%)	2/2 (100%)
	2nd	21/22 (95.45%)	20/20 (100%)	1/2 (50%)
Radiologist 2	1st	19/22 (86.36%)	17/20 (85%)	2/2 (100%)
	2nd	22/22 (100%)	20/20 (100%)	2/2 (100%)
Radiologist 3	1st	14/22 (63.64%)	12/20 (60%)	2/2 (100%)
	2nd	18/22 (81.82%)	16/20 (80%)	2/2 (100%)

Among the 20 definite MPM cases, the cases with MPM probability Grade 2, Grade 3 and Grade 4 accounted for 3/20 (15%), 7/20 (35%) and 10/20 (50%), respectively.

For the 3 cases with MPM probability Grade 2, the cases with the feature "nodular pleural thickening" ("nt") accounted for 1/3(33.33%), and the cases with "invasion" ("iv") accounted for 2/3 (66.67%).

Among the 7 cases with MPM probability Grade 3, the cases with feature "medialstinal pleural thickening" ("mt") accounted for 7/7 (100%), the feature of "unilateral pleural effusion" ("ue") were present in 5/7 (71.43%), "interlobar fissure thickening" ("it") in 4/7 (57.14%), "diminished lung" ("dl") in 4/7 (57.14%), "nt" in 2/7 (28.57%), and "iv" in 1/7 (14.29%).

Among the 10 cases with MPM probability Grade 4, the most frequently recorded features were "nt" in 10/10 (100%), "mt" in 100%, and "dl" in 100%. The cases with feature "ue" were in 80%, "it" in 70%, "iv" in 60%, and "tumoral encasement of lung" in 50%.

3.2. The sensitivity and specificity for MPM by three radiologists, the agreement on MPM probability by radiologists with experts

The sensitivity for MPM, specificity for MPM and observed agreement on the dichotomized MPM probability by 3 radiologists at two times of CT readings before and after studying the MPM-CT Guideline are shown as in Table 2.

The sensitivity for MPM by the three radiologists at the 2nd trial was 100%, 100% and 80%, which was higher than 80%, 85% and 60%, respectively at the 1st reading trial. The observed agreements on dichotomized MPM probability by radiologists were increased at the 2nd trial compared with those at the 1st trial.

The values of weighted kappa for the agreement of MPM probability on the 4-point scale by three radiologists with experts were increased at the 2nd trial, compared with those at the 1st trial, as shown in Table 3.

The weighted kappa values for the agreement with experts on 4-point scale MPM probability by three radiologists were 0.32, 0.51 and 0.37 at the 2nd trial vs 0.24, 0.48 and 0.29 at the 1st trial, respectively. The kappa value for inter-reader agreements on the dichotomized MPM probability between radiologists and experts at the 2nd reading trial were 0.65 (good), 1 (excellent) and 0.42 (moderate), respectively, which were significantly higher than 0.42 (moderate), 0.51 (moderate) and 0.21 (fair) at the 1st trial, respectively. The average kappa for the agreement on dichotomized MPM probability between radiologists and experts were 0.69 (good) at the 2nd trial vs 0.38 (fair) at the 1st trial, which seemed to show an upgrading in reading skill.

3.3. The agreement on MPM features between radiologists and experts

The results of the agreements for the recorded MPM features between the three radiologists and experts are shown as in Table 4.

For radiologist 1, the agreement with experts for 6 features "unilateral pleural effusion" ("ue"), "nodular pleural thickening" ("nt"), "interlobar fissure thickening"("it"), "mediastinal pleural thickening" ("mt"), "invasion" ("iv") and "diminished lung" ("dl") at the 2nd reading trial was better compared with those at the 1st trial. The agreement for feature "ue" and "nt" at the 2nd trial was good (kappa = 0.62 and 0.61, respectively). The agreement for feature "tumoral encasement of lung" ("te") at the 2nd trial was excellent to the same extent as that at the 1st trial (kappa = 0.86). The agreement with experts on 3 features ("mt", "iv" and "dl") was markedly increased to excellent (kappa > 0.8) at the 2nd trial.

For radiologist 2, the kappa values for the agreement with experts were increased for 5 features ("ue", "nt", "mt", "te" and "dl") at the 2nd trial in comparison with those at the 1st trial. The kappa values for the features "ue", "nt" and "te" showed good agreement with experts (kappa > 0.6), and "mt" and "dl" showed excellent agreement (kappa > 0.8). The kappa values for the feature "it" and "iv" was 0.55 and 0.51 at the 2nd trial, which were lower than 0.73 and 0.61 at the 1st trial, respectively.

For the radiologist 3, the kappa values for 5 features ("nt", "mt", "te", "iv" and "dl") were increased at the 2nd trial in comparison with the 1st trial. The feature "nt" and "te" shows good agreement with expert (kappa = 0.64 and 0.77, respectively). The kappa value for the feature "it" at the 2nd trial was equal to that one at the 1st trial. The kappa value for the feature "ue" (0.49) at the 2nd trial was lower than at the 1st trial (0.65).

The average kappa values of 7 MPM CT features at the 2nd trial by the three radiologists were significantly increased in comparison with the 1st trial, and the six features "ue", "nt", "mt", "te" and "dl" showed good agreement between radiologists and experts (kappa > 0.60).

Table 5 shows that the kappa values for the agreement on the 7 MPM CT features by the three radiologists with experts were significantly higher than those at the 1st trial.

Table 3
Agreement on 4-point scale MPM probability and dichotomized MPM probability between radiologist and experts in terms of weighted kappa.

Reader	4-scale MPM probability K_w (95% CI)		Dichotomized MPM probability K_w (95% CI)	
	1st trial	2nd trial	1st trial	2nd trial
Radiologist 1	0.24 (−0.06, 0.54)	0.32 (0.06, 0.58)	0.42 (−0.09, 0.93)	0.65 (−0.03, 1)
Radiologist 2	0.48 (0.19, 0.76)	0.51 (0.24, 0.78)	0.51 (−0.01, 1)	1
Radiologist 3	0.29 (0.04, 0.53)	0.37 (0.12, 0.62)	0.21 (−0.22, 0.65)	0.42 (−0.09, 0.93)
Weighted kappa Mean(SD)	0.34 (0.13)	0.40 (0.10)	0.38(0.15)	0.69(0.29)

Table 4
Agreement for the recorded MPM CT features between radiologists and experts by kappa statistics.

Reader	Reading trial	Experts						
		ue	nt	it	mt	te	iv	dl
Radiologist 1	1st	0.32	0.35	0.36	0.20	0.86	0.25	0.49
	2nd	0.62	0.61	0.55	0.88	0.86	0.81	0.80
Radiologist 2	1st	0.65	0.31	0.73	0.68	0.60	0.61	0.73
	2nd	0.72	0.70	0.55	1	0.77	0.51	0.90
Radiologist 3	1st	0.65	0.37	0.45	0.39	0.28	0.25	0.17
	2nd	0.49	0.64	0.45	0.47	0.77	0.49	0.57
All radiologists Mean (SD)	1st	0.54 (0.19)	0.34 (0.03)	0.51 (0.19)	0.42 (0.24)	0.58 (0.29)	0.37 (0.21)	0.46 (0.28)
All radiologists Mean(SD)	2nd	0.61 (0.12)	0.65 (0.05)	0.52 (0.06)	0.78 (0.28)	0.80 (0.05)	0.60 (0.18)	0.76 (0.17)

Note: 1st and 2nd indicates the 1st CT reading trial and the 2nd CT reading trial, SD = standard deviation of kappa values.

Table 5
Comparative analysis for the kappa values for the agreement with experts on the 7 MPM CT features by all three radiologists between the two reading trials by means of 2-Related-Samples Nonparametric Test (Wicoxon Signed Rank Test).

Kappa 2–Kappa 1*	Number of pairs	Mean rank	Sum of ranks	*P*
Negative ranks[a]	3	4.67	14	<0.01
Positive ranks[b]	16	11	176	
Ties[c]	2			
Total	21			

Note: *Kappa 2: kappa value for the agreement by three radiologists with expert on the 7 features recorded at the 2nd reading trial. Kappa 1: kappa value for the agreement by three radiologists with expert on the 7 features recorded at the 1st reading trial.

[a] Kappa 2 < Kappa 1.
[b] Kappa 2 > Kappa 1.
[c] Kappa 2 = Kappa 1.

4. Discussion

With the development of modern technology, CT scans have now become routine clinical practice for detecting pleural abnormalities in patients. The diagnosis of MPM is usually based on the combination of occupational history, physical and laboratory examination, radiology and the thoracic pathology. CT findings are important to provide the clue in the diagnosis of MPM before any invasive biopsy procedures take place. Diagnosis of MPM at the early stage may enable patients to obtain a better outcome with multiple modality therapy including extensive surgery, chemotherapy, and radiotherapy, which may offer increases in survival time and the life quality for MPM patients [7].

The MPM-CT Guideline was developed by the international experts' efforts [2]. The Guideline provided a standardized way for physicians to record CT findings on subject CT films with the assistance of the MPM reference CT films with typical MPM features. These allow the physicians to make appropriate judgments for the MPM probability, which is determined by the overall impression of the CT findings as a whole and comprehensive evaluation on CT findings being consistent or inconsistent with MPM features, the severity of the diseases, and the distribution of MPM involvement.

Among the 20 definite MPM cases in the current study, the mostly seen features in the number were "mediastinal pleural thickening" ("mt") (85%), and then were "diminished lung" ("dl") (70%), the "unilateral pleural effusion" ("ue") (65%), "nodular pleural thickening" ("nt") (65%) and "interlobar fissure thickening" ("it") (55%). The cases with "invasion" accounted for 45%. Most of the 7 features are suggestive of MPM to somewhat through quite extent and frequently common on the CT images of MPM [8].

The relationship between the MPM probability and the number of 7-MPM-CT features in each case was investigated. Among the 20 MPM cases, those cases with the high MPM probability (Grade 3, 4) were found to have more of 7-MPM-CT features. It was suggested that the more features observed on the CT, the higher MPM probability for the case determined, presenting with a positive correlation. The severity in association with the feature may be the second reason related with probability of MPM. When the features are at severe disease stages, the cases may have high MPM probability, even with only a few features of these.

The relatively high prevalence and frequency of "unilateral pleural effusion" in MPM is of major diagnostic importance [9]. At the early stage of MPM, irrespective of normal-appearing pleura, "unilateral pleural effusion" can be the only finding. The main mechanism of pleural fluid formation in malignancy is lymphatic obstruction. For the cases with pleural effusion and a history of asbestos exposure, MPM should be considered and further investigation should be conducted [10].

There were two features listed in the MPM-CT Guideline "contracted hemithorax" ("ch") and "pleural mass" ("pm") not included in the current comparative analysis, because these two features were later added at the 2nd workshop to the proposed MPM-CT Guideline. The two features are crucial and helpful to make diagnosis of MPM. Solitary masses may occur at the early stage, while multiple masses are more common at later stages [11]. MPM tend to spread along the pleural surface in a "sheet-like" fashion [12]. In CT images with feature "ch", the involved hemithorax is noticeably contracted from a comparison with that in the contralateral lung.

The current study showed that after studying the MPM-CT Guideline, the sensitivity for MPM by all three radiologists was

increased at the 2nd trial compared with those at the 1st trial. For the 1st radiologist, although the specificity for MPM at the 2nd trial was lower than at the 1st trial, the observed agreement for the MPM probability was increased to 95.45% at the 2nd trial vs 81.82% at the 1st trial.

Kappa is affected by prevalence of the finding under observation [13,14]. In the current study, the proportion of the non-MPM cases among total case was only in 10%, and many cases (50%) had MPM probability Grade 2 or Grade 3, which had great variances between readers. Therefore the weighted kappa on 4-scale MPM probability proved to be low. However, the analysis with the dichotomized MPM probability showed that two radiologists obtained good and excellent agreements, i.e., kappa = 0.65 and 1, respectively. The 3rd radiologist had achieved moderate agreement with kappa 0.42 on dichotomized MPM probability at the 2nd trial vs kappa 0.21 at the 1st trial.

The kappa statistics showed that good through to excellent agreements with experts by two of the three radiologists were obtained at the 2nd trial for 5 and 6 features, respectively. For the radiologist 3, there were 5 features including "nt", "mt", "tumoral encasement of lung" ("te"), "invasion" ("iv") and "dl" with increased agreements with experts at the 2nd trial compared with those at the 1st trial. Compared with those at the 1st trial, the average kappa values of 7 features by the three radiologists were increased at the 2nd trial, in which the five features, i.e., "ue", "nt", "mt", "te" and "dl", showed good agreement with experts. Wicoxon Signed Rank Test showed that the kappa values for the agreement on the 7 MPM CT features between the three radiologists and experts were significantly higher than those at the 1st trial. These revealed that the radiologists had made improvement in recognition of the MPM CT features at the 2nd trial compared with the 1st trial.

Compared to the other features in the 20 MPM cases, the agreement with experts in the feature "invasion" was relatively lower. At the 2nd trial, the kappa for "invasion" was 0.51 by the 2nd radiologist and 0.49 by the 3rd radiologist, respectively. This implied that the feature "invasion" was difficult to identify compared to the other MPM features. One reason may be its frequent coexistence with other features that the appearance of this feature may become less notable. The severity of the invasion to the lung structure may be the second reason. If it was less severe, "invasion" may not be easy to identify. This feature of "invasion" is quite suggestive of malignancy. This feature overlaps with metastasis of other carcinoma [15], while the other malignancy also has lung parenchymal involvement.

The average kappa for the agreements between radiologists and experts on feature "interlobar fissure thickening" was 0.51 and 0.52 at the 1st and 2nd trials, respectively, which were lower than those of other features. The reason may be ascribed to the fact that "interlobar fissure thickening" in some cases is so slight that it may easily be neglected. The feature "interlobar fissure thickening" reflects tumor growth along the interlobar spaces, and may represent one of the earliest significant MPM features, which is seen less frequently in other malignancies or in benign pleural diseases [16].

The CT findings in MPM are not pathognomonic because similar findings may be found in metastatic carcinoma. Nevertheless, they are characteristic. The MPM features can provide valuable information to make a diagnosis of MPM. By identifying the MPM features on CT images, clinicians can recognize MPM [17]. It will be helpful for occupational physicians during the occupational disease screening in health surveillance for workers.

One limitation of the study was that there were only two non-MPM cases with pleural plaque. This may affect the specificity for MPM. Despite the limitation, the results of the comparative study showed that all three radiologists had improved their sensitivity for MPM after studying the MPM-CT Guideline. Two of them had obtained either good or excellent agreements with experts in identifying most of features at the 2nd trial. These suggested that reliability of the Guideline and the MPM reference CT films to improve the reading proficiency of the radiologists may be validated.

5. Conclusions

The current study suggested that the three radiologists improved the proficiency in diagnosis for MPM by identifying of MPM CT features after studying the MPM-CT Guideline with reference MPM CT features. The MPM-CT Guideline and reference CT films may act as good tool to facilitate physicians in recognition of MPM features and contribute to early diagnosis of MPM in the health surveillance.

Conflict of interest statement

None of the authors has a financial relationship with a commercial entity that has an interest in the subject of this manuscript.

Role of the funding source

This study was supported by a grant from the Ministry of Education, Sports, Culture, Science and Technology, Japan. The fundholder had no involvement in the study design, collection and analysis and interpretation of data or in the writing of manuscript and in the decision to submit the manuscript for publication.

Acknowledgments

The author gratefully acknowledge all concerned: Dr. Mitsunori Sakatani, Dr. Seiji Hayashi, Dr. Giichi Inoue, Dr. Masanori Kitaichi, National Hospital Organization Kinki-Chuo Chest Medical Center, Osaka, Japan; Prof. Hisao Shida, Committee of Compensation of Asbestos Related Diseases, Ministry of the Environment Protection, Kawasaki, Japan; Dr. Norihiko Hamada, Department of Radiology, Kochi University, Japan; and we also express thanks to the bereaved family of the patient of MPM and other abnormalities to provide us with the valuable information.

Appendix A. Supplementary data

Supplementary data associated with this article can be found, in the online version, at http://dx.doi.org/10.1016/j.ejrad.2012.05.022.

References

[1] Kusaka Y, Hering KG, Parker JE, editors. International classification of HRCT for occupational and environmental respiratory diseases. Tokyo: Springer-Verlag; 2005.
[2] Zhou H, Tamura T, Kusaka Y, et al. Development of the guideline on reading CT images of malignant pleural mesothelioma and selection of the reference CT films. European Journal of Radiology 2012, http://dx.doi.org/10.1016/j.ejrad.2012.08.008.
[3] Kurumatani N, Kumagai S. Mapping the risk of mesothelioma due to neighborhood asbestos exposure. American Journal of Respiratory and Critical Care Medicine 2008;178:624–9.
[4] Inai K. Pathology of mesothelioma. Environmental Health and Preventive Medicine 2008;13:60–4.
[5] International Mesothelioma Interest Group. A proposed new international TNM staging system for malignant pleural mesothelioma. Chest 1995;108:1122–8.
[6] Suganuma N, Kusaka Y, Hering KG, et al. Reliability of the proposed international classification of high-resolution computed tomography for occupational and environmental disease. Journal of Occupational Health 2009;51:210–22.
[7] Sterman DH, Albelda SM. Advances in the diagnosis, evaluation, and management of malignant pleural mesothelioma. Respirology 2005;10:266–83.
[8] Yamamuro M, Gerbaudo VH, Gill RR, Jacobson FL, Sugarbaker DJ, Hatabu H. Morphologic and functional imaging of malignant pleural mesothelioma. European Journal of Radiology 2007;64:356–66.

[9] Kawashima A, Libshitz HI. Malignant pleural mesothelioma: CT manifestations in 50 cases. American Journal of Roentgenology 1990;155:965–9.
[10] Fujimoto N, Aoe K, Gemba K, Kato K, Amazaki K, Kishimoto T. Clinical investigation of malignant mesothelioma in Japan. Journal of Cancer Research and Clinical Oncology 2010;136:1755–9.
[11] Yilmaz UM, Utkaner G, Yalniz E, Kumcuoglu Z. Computed tomographic findings of environmental asbestos-related malignant pleural mesothelioma. Respirology 1998;3:33–8.
[12] Miller BH, Rosado-de-Christenson ML, Mason AC, Fleming MV, White CC, Krasna MJ. From the archives of the AFIP malignant pleural mesothelioma: radiologic-pathologic correlation. Radiographics 1996;16:613–44.
[13] Viera AJ, Garrett JM. Understanding interobserver agreement: the kappa statistic. Family Medicine 2005;37(5):360–3.
[14] Feinstein AR, Cicchetti DV. High agreement but low kappa: I. The problems of two paradoxes. Journal of Clinical Epidemiology 1990;43:543–9.
[15] Leung AN, Müller NL, Miller RR. CT in differential diagnosis of diffuse pleural disease. American Journal of Roentgenology 1990;154:487–92.
[16] Knuuttila A, Kivisaari L, Kivisaari A, Palomäki M, Tervahartiala P, Mattson K. Evaluation of pleural disease using MR and CT with special reference to malignant pleural mesothelioma. Acta Radiologica 2001;42:502–7.
[17] Metintas M, Ucgun I, Elbek O, et al. Computed tomography features in malignant pleural mesothelioma and other commonly seen pleural diseases. European Journal of Radiology 2002;41:1–9.

Ninomiya et al. BMC Cancer 2013, 13:8
http://www.biomedcentral.com/1471-2407/13/8

BMC Cancer

RESEARCH ARTICLE Open Access

Allelotypes of lung adenocarcinomas featuring *ALK* fusion demonstrate fewer onco- and suppressor gene changes

Hironori Ninomiya[1], Motohiro Kato[4,5], Masashi Sanada[4], Kengo Takeuchi[1,2], Kentaro Inamura[1], Noriko Motoi[1], Hiroko Nagano[1], Kimie Nomura[1], Yukinori Sakao[3], Sakae Okumura[3], Hiroyuki Mano[6,7], Seishi Ogawa[4] and Yuichi Ishikawa[1*]

Abstract

Background: A subset of lung adenocarcinomas harboring an *EML4-ALK* fusion gene resulting in dominant oncogenic activity has emerged as a target for specific therapy. *EML4-ALK* fusion confers a characteristic histology and is detected more frequently in never or light smokers and younger patients.

Methods: To gain insights into etiology and carcinogenic mechanisms we conducted analyses to compare allelotypes of 35 *ALK* fusion-positive and 95 -negative tumours using single nucleotide polymorphism (SNP) arrays and especially designed software which enabled precise global genomic profiling.

Results: Overall aberration numbers (gains + losses) of chromosomal alterations were 8.42 and 9.56 in tumours with and without *ALK* fusion, respectively, the difference not being statistically significant, although patterns of gain and loss were distinct. Interestingly, among selected genomic regions, oncogene-related examples such as 1p34.3 (*MYCL1*), 7q11.2(*EGFR*), 7p21.1, 8q24.21(*MYC*), 16p13.3, 17q12(*ERBB2*) and 17q25.1 showed significantly less gain. Also, changes in tumour suppressor gene-related regions, such as 9p21.3 (*CDKN2A*) 9p23-24.1 (*PTPRD*), 13q14.2 (*RB1*), were significantly fewer in tumours with *ALK* fusion.

Conclusion: Global genomic comparison with SNP arrays showed tumours with *ALK* fusion to have fewer alterations in oncogenes and suppressor genes despite a similar overall aberration frequency, suggesting very strong oncogenic potency of *ALK* activation by gene fusion.

Keywords: Lung adenocarcinoma, *ALK* fusion, SNP array, Allelotype, Copy number

Background

The adenocarcinoma is the most common form of lung cancer worldwide, different subsets having specific genetic backgrounds of great importance for molecular-targeted therapy. For example, somatic mutations of the epidermal growth factor receptor (*EGFR*) are especially prevalent in adenocarcinomas among never smokers, females, and those with Asian ethnicity [1]. On the other hand, *KRAS* mutations are associated with the smoking habit [2] and the two tend to be mutually exclusive. Recently, Soda et al. found a novel fusion gene, *EML4-ALK*, arising from an inversion on the short arm of chromosome 2 in non-small cell lung carcinomas [3]. *ALK* fusion is a unique example of tyrosine kinase activation by structural chromosome rearrangement [4].

EML4-ALK fusion is a powerful driving molecular event by itself. The chimeric protein permits ligand-independent dimerization and constitutive activation of *ALK*, resulting in dominant oncogenic activity. Multiple fusion variants of *EML4-ALK* and notable clinicopathological characteristics of fusion positive tumours have been revealed [5-9]. Since the tyrosine kinase is involved and activated by gene fusion, this type of malignancy has emerged as a target for anti-tyrosine kinase therapy [4,10-12].

We have revealed that *ALK* fusion-positive tumours constituted a particular subset in lung adenocarcinomas in

* Correspondence: ishikawa@jfcr.or.jp
[1]Division of Pathology, The Cancer Institute, Ariake 3-8-31, Koutou-ku, Tokyo 135-8550, Japan
Full list of author information is available at the end of the article

terms of clinical characteristics, histology and etiology, as well as molecular changes [7,8]. It is of great interest to assess global genomic alterations to provide deep insight into their genesis, especially considering these tumours arise in non- or light smokers. Single nucleotide polymorphism (SNP) microarray analysis enables precise high-throughput detection of genomic copy number alterations, gains and losses in the genome contributing to carcinogenesis [13] with gene expression varying consistently with DNA copy number changes [14,15]. We therefore conducted of the present genomic profiling of lung adenocarcinomas with and without *ALK* fusion.

Methods

Patient population and specimens

A series of 130 cases of lung adenocarcinomas, 35 with *EML4-ALK* or *KIF5B-ALK* fusion and 95 cases without, were enrolled in this study. From 1998 to 2008, 1,086 primary lung adenocarcinomas were surgically resected at Thoracic Surgery Division, the Cancer Institute Hospital, Japanese Foundation for Cancer Research (JFCR), Tokyo. All cases were screened as to ALK expression by immunohistochemistry using the iAEP method [6] and for positive cases subsequent RT-PCR and FISH analysis were performed, as previously described [5,6,16]. Among them, sufficient amounts and quality of fresh tumour material were available for 35 cases. Fusion gene variants are listed in Addtional file 1: Table S1. V3 constituted the largest proportion, 31% (11/35), having a breakpoint at exon 20 of *EML4*. A rare variant, *KIF5B-ALK* fusion, was detected in two cases. There was no correlation with fusion variant and pathological subtypes (data not shown). The 95 cases without *ALK* fusion were randomly selected from 730 surgically resected adenocarcinomas from 1995 to 2003 at the same hospital. Tissue specimens were snap-frozen in liquid nitrogen, typically within 20 minutes after resection, and stored at −80°C until use. Genomic DNA was extracted by standard proteinase K digestion and the phenol-chloroform method. To confirm if specimens used for analysis in this study contained a significant amount of tumour cells, typically 50% or more, a neighboring surface was examined histologically with frozen sections. This study was approved by the institutional review board of the JFCR.

Mutation analysis of EGFR, KRAS and TP53

For *EGFR* mutation analysis, exons 18 to 21 were amplified by PCR with specific oligo-primers. For point mutations in exon 18, PCR products were directly sequenced. Fragment analysis was performed for exons 19 and 20 deletions and insertion mutations. The presence of one point mutation in exon 21 was detected by genotyping analysis. To examine *TP53* mutations, direct sequencing from exons 5 to 10 was carried out. For *KRAS* mutation analysis, codons 12, 13 and 61 were examined by direct sequencing. Primers and detailed procedures were as described previously [17].

Histological diagnosis and clinical staging

Histological diagnosis was made on the basis of World Health Organization (WHO) classification [18] by experienced pathologists (N.M. and Y.I.). Pathological staging was based on the AJCC/UICC staging manual of lung cancer [19]. Differentiation grading of adenocarcinoma was determined essentially according to the Japan Lung Cancer Society criteria as illustrated previously [20]. Briefly, well-differentiated (w/d) tumors are composed chiefly of glands lined by, or of papilla covered by, one-layered tumor cells. Also, Adenocarcinoma in situ (AIS) is included in this category. Moderately differentiated (m/d) lesions comprise glands showing a cribriform pattern, fused with one another, or glands lined by, or papillae covered by, tumor cells demonstrating obvious piling-up. Poorly differentiated (p/d) carcinomas show mainly solid growth and only occasionally glandular/papillary patterns and/or mucus production. Blood vessel and lymphatic invasion was also explored microscopically, with hematoxylin-eosin and elastic-fiber stained sections of maximum tumour diameter made from paraffin-embedded specimens.

SNP array analysis and comparisons of allelic imbalance at the chromosome arm level and in selected cancer-related regions

Extracted DNA was subjected to Affymetrix GeneChip Mapping 250K arrays. Allelic imbalance was analyzed using software termed the Copy Number Analyzer for Affymetrix Gene Chip Mapping (CNAG Ver. 2.0) [21]. After appropriate normalization of mean array intensities, signal ratios between tumours and anonymous normal references were calculated in an allele-specific manner, and allele-specific copy numbers were inferred from the observed signal ratios based on the hidden Markov model using the CNAG/AsCNAR software [21-23]. With this procedure, genomic profiles of *ALK* fusion-positive and -negative tumours were obtained. Datas have been deposited at NCBI's Gene Expression Omnibus data repository under GEO series accession number GSE41536.

Comparison was at two levels; a chromosome arm level and a smaller, specific gene locus level. To do this, first we compared average numbers of chromosome arms altered between the two groups [24]. We called gain or loss of each chromosomal arm when copy number change stretched more than 80% of entire length. Secondly, we compared recurrent copy number aberrations at twenty-one cancer-related loci with gains and five with losses. These specific regions were selected based on previous studies of the lung cancer genome

[25,26] and through our global mapping with CNAG. The selected regions with relevant genes were as follows: for gains, 1p34.3 (*MYCL1*), 1q21.2 (*S100 family*), 3q29 (*MUC4*), 5p15.33 (*TERT*), 6p21.1 (*VEGF*), 7p11.2 (*EGFR*), 7p21.1, 7q31.2 (*MET*), 8q24.21 (*MYC*), 10q11.22, 12p12.1 (*KRAS*), 12q14.1 (*CDK4*), 12q15 (*MDM2*), 14q13.3 (*TTF1*), 16p13.3, 17q12 (*ERBB2*), 17q25.1, 19q12 (*CCNE1*), 20q13.2, 20q13.32, 20q13.33 (*TNFSF6B*); and for losses, 9p21.3 (*CDKN2A*), 9p23-p24.1 (*PTPRD*), 10q23.31 (*PTEN*), 13q14 (*RB1*), 17p13.1 (*TP53*).

Statistical analysis

Clinicopathological parameters of cases with or without *ALK* fusion and the frequencies of chromosome arms changed and copy numbers of targeted loci were compared by the chi-square test or the Fisher's exact test as appropriate. The average number of chromosome arms altered with or without *ALK* fusion was compared with Students' *t*-test. Statistical significance was defined as P=0.05 or less.

Results

Comparisons of clinicopathological profiles of tumours with or without *ALK* fusion

Clinicopathological profiles of patients are summarized in Table 1. *ALK* fusion-positive cases were significantly younger and featured significantly more never-smokers (P=0.05, P=0.004, respectively). *ALK* fusion-positive tumours were histologically adenocarcinomas with notable characteristics such as poor differentiation as well as an acinar type structure and mucin production, as reported previously [7-9]. In this study, distribution of histological subtypes differed between two groups, namely, "acinar" subtype accounted for nearly forty percent in *ALK* fusion positive group (Table 1). The frequencies of vascular invasion, both of blood and lymph vessels, did not significantly differ between the two groups (P=0.738, P=0.273, respectively). In addition, the distribution of pathological stages did not vary (P=0.532).

Table 1 Comparison of clinicopathological parameters in cases with or without ALK fusion

	with fusion	without fusion	*P*
n	35	95	
Age (years)	58.5	62.8	0.050
gender			
male	14	47	0.337
female	21	48	
smoking			
never	25	41	0.004
ever	10	54	
pStage			
I	20	60	0.532
II-IV	15	35	
differentiation grade			
wel	4	44	<0.001
mod+por	31	51	
Predominant subtype			
papillary	21	77	0.019
Acinar	13	13	
Bronchioloalveolar	0	4	
solid with mucin	0	1	
signet	1	0	
lymphatic invasion			
-	24	68	0.738
+	11	27	
Vessel invasion			
-	15	51	0.273
+	20	44	
TP53 mutation			
-	34	75	0.014
+	1	20	
EGFR mutation			
-	35	40	<0.0001
+	0	55	
KRAS mutation			
-	35	88	0.189
+	0	7	

Mutational status of TP53, EGFR and KRAS

Data for the mutational status of *TP53, EGFR and KRAS* in the two groups are summarized in Table 1. Twenty-one cases had *TP53* mutations. Only one case with *ALK* fusion (Case 9: 1/35, 3%) harbored a mutation, a G/A transition at codon 273, as compared to 20 cases without *ALK* fusion (20/95, 21%), the mutation rates being significantly different (P=0.014) (Table 1, Additional file 1: Table S2). Twelve (12/21, 57%) of the *TP53*-mutated cases had a smoking history.

EGFR and *KRAS* mutations were not detected among *ALK* fusion-positive tumours. This fact that *ALK* rearrangement was mutually exclusive with *EGFR* and *KRAS* mutations (P<0.0001, P=0.189, respectively) is in line with our previous studies [8]. The *EGFR* mutation rate was 58% (55/95) in *ALK* fusion-negative cases and decreased with the smoking burden: 70.7% (29/41) in never smokers, 62.5% (15/24) in light smokers (0<pack-years<20) and 36.7% in heavy smokers (more than 20 pack-years) (11/30) (Additional file 2: Figure S1). *KRAS* mutations were identified in 7.4% (7/95) of *ALK* fusion-negative cases, and detected only among smokers. Though *KRAS* mutations were examined through

codons 12, 13 and 61, they were found only in codon 12. The *KRAS* mutation rate increased along with the elevation of smoking index (Additional file 2: Figure S1). These findings for *EGFR* and *KRAS* mutations are consistent with previous reports from Japan, the prevalence being quite different from that in the United States [27-29].

DNA copy number alterations of chromosome arms

We compared the allelotypes of each chromosome arm between the two groups. Global views of chromosome aberrations are shown in Figure 1. Note that in *ALK* fusion-positive tumours, genomic copy number changes were more evenly distributed over the chromosome arms and high copy number gains (dark-red) in short genomic segments were less frequently encountered than with *ALK*-fusion negative examples. Significantly different patterns of respective chromosomal arm gain and loss were noted between the two groups. In fact, 5q, 8p, 9q, 11p and 11q were significantly more amplified, and 6q was more deleted in *ALK* fusion-positive tumours, whereas, in *ALK* fusion-negative tumours, 17q was more amplified, and 8p and 9p were more deleted (Figure 1, Table 2a, Additional file 1: Table S3-S5). *P*-values for comparisons of the aberration frequency in each chromosome arms are shown in Additional file 1: Table S5. When comparing global chromosome instability levels between the two groups, average numbers of chromosome arms with copy number gain or loss were 8.42 ±7.46 and 9.56 ±7.90 for tumours with and without *ALK* fusion, respectively, as detailed in Table 3, the difference not being statistically significant.

Chromosomal number alterations with advancement of pathological stage

Chromosome aberration might be expected to increase as tumours progress in stages and, if so, numbers of chromosome arms with gain and/or loss might be larger in advanced tumours. In fact however, when we compared the number of chromosome arm altered between pathological stage I and II-IV, total number did not increase in pathological stage II-IV, though only *ALK* fusion-negative tumours showing significant elevation of chromosomal gain (Figure 2).

Comparison of gain and loss frequency of selected loci

We selected twenty-one loci with recurrent copy number gain and five loci with loss to compare small-scale genomic aberrations. All the loci examined and *P*-values are summarized in Additional file 1: Table S6, S7. In Figure 3, stacked bar charts are shown indicating the

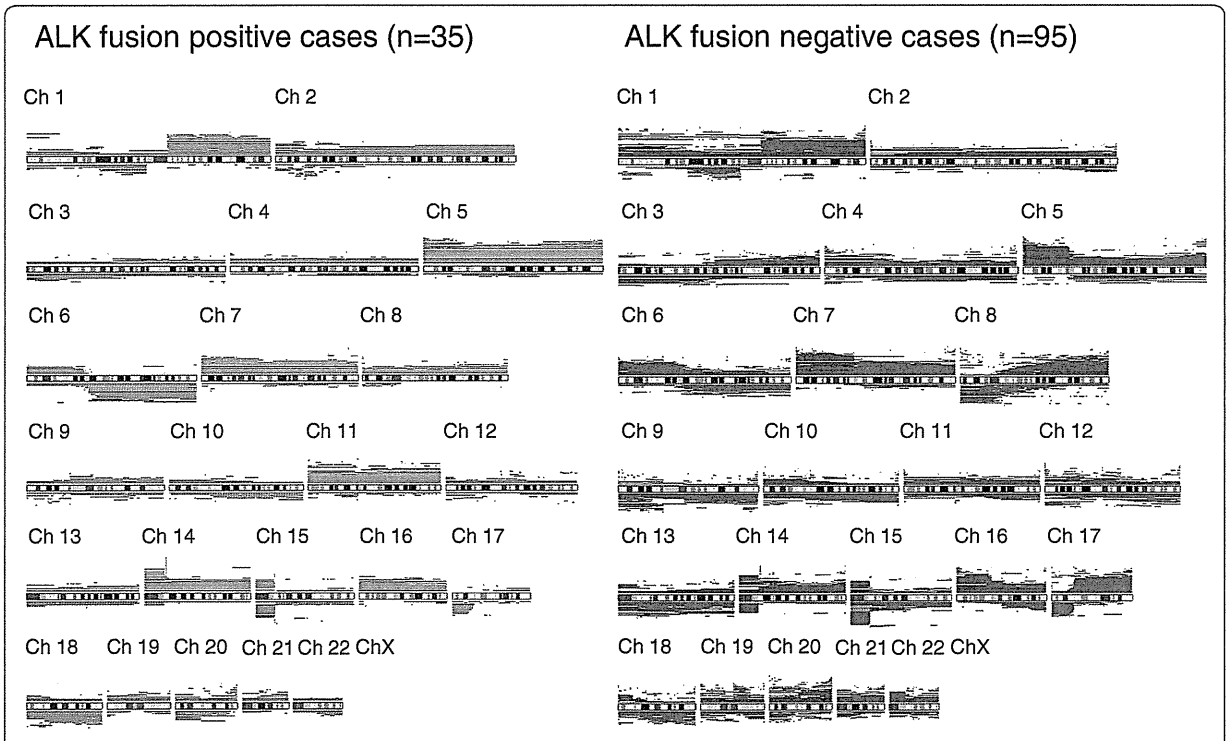

Figure 1 Global view of copy number alterations with or without *ALK* fusion. A line above a chromosome represents one case with genomic gain and its length. The color indicates the copy number of genomic regions: pink, 3 or 4 copies; and dark-red, ≥ 5 copies. Lines beneath the chromosomes represent copy number loss: blue, 1 copy; and light-green, 2 copies (homozygous deletion). Width between the lines of the two groups are adjusted according to the number of cases included for ease of visual comparison.

Table 2 Comparisons of significantly altered chromosomal arms between adenocarcinomas with and without *ALK* fusion

Category	Gain	Loss
More frequent *with* ALK fusion	5q, 8p, 9q, 11p, 11q	6q
More frequent *without* ALK fusion	17q	8p, 9q

percentage gain or loss of the selected loci. Interestingly, copy numbers (and related genes) at 1p34.3 (*MYCL1*), 7p11.2 (*EGFR*), 7p21.1, 8q24.21 (*MYC*), 16p13.3, 17q12 (*ERBB2*) and 17q25.1 were significantly less gained, and those at 9p21.3 (*CDKN2A*), 9p23-p24.1 (*PTPRD*), 13q14.2 (*RB1*) were significantly less deleted in *ALK* fusion-positive tumours than fusion-negative ones, with loci related to both oncogenes and tumour suppressor genes having fewer changes in tumours with *ALK* fusion. There were no oncogene-related loci with more gains and no suppressor gene-related loci with more losses in tumours with *ALK* fusion.

Homozygous deletions were found only at 9p21, at frequencies similar between the two groups, although the summed frequencies of heterozygous and homozygous deletions at 9p21.3 did significantly differ. In the group without *ALK* fusion, all the cases with the homozygous deletion harbored *EGFR* mutations.

MYCL1, EGFR, MYC and *ERBB2* are well-known oncogenes and *CDKN2A* and *RB1* are tumour suppressor genes related to lung carcinogenesis. *PTPRD* has been suggested to function as a tumour suppressor in several tumours, including lung cancers [30] and brain tumours [31]. Notably, 5p15.33, including *TERT* (telomerase reverse transcriptase), had the highest rate of gain in both groups regardless of *ALK* fusion (Additional file 3: Figure S2 and Additional file 1: Table S7).

Taken together, *ALK* fusion-positive tumours showed similar levels of overall chromosome instability, but when focusing on particular cancer-related regions, significantly fewer copy number gains at oncogene-related loci and significantly fewer deletions at suppressor gene-related loci.

Discussion

Recurrent chromosome translocation has been accepted to play an important role in the pathogenesis of hematological malignancies, but not of solid tumours. Recently, however, chromosome rearrangements in solid tumours such as prostate cancer and non-small cell lung cancer have been reported [32]. *ALK* fusion was originally described in anaplastic large-cell lymphoma as a chimeric protein *NPM-ALK* resulting from a translocation. More recently, evidence has accumulated that the *EML4-ALK* fusion gene defines a novel subclass of lung adenocarcinomas with distinct clinicopathological features [7-9], so that it has emerged as a target for therapy. We focused here for the first time on allelic imbalance of tumours with *ALK* fusion with a novel technique which has already shown the involvement of loss of A20 function in the pathogenesis of a subset of B-cell lymphomas [33] and gain of function of C-CBL tumour suppressor in myeloid neoplasms [34]. Applying this methodology, we demonstrated that lung adenocarcnomas with *ALK* fusion feature less amplification of loci with oncogenes and fewer deletions of loci related to tumour suppressor genes, although global chromosome aberrations were similar between tumours with and without *ALK* fusion. suggesting that the fusion gene is a driver mutation, not just a passenger mutation.

Table 3 Comparisons of numbers of chromosome arms with aberrations between adenocarcinomas with or without *ALK* fusion

	with *ALK* fusion (n=35)	without *ALK* fusion (n=95)	*P*
Gains	5.97±6.75	6.21±6.95	0.859
Losses	2.46±3.06	3.35±4.34	0.196
Total	8.42±7.46	9.56±7.90	0.454

Note that significant differences are not detected.

Genetic instability was here categorized into two groups for simplicity, at the chromosomal level and at the nucleotide level. We earlier found the former to play a more important role in lung carcinogenesis, the frequency of LOH (loss of heterozygosity) being higher in less-differentiated tumours [35]. *ALK* fusion positive tumours are more common among non-smokers and the younger population, similar to those with *EGFR* mutations. We had expected fewer chromosome aberrations in *ALK* fusion-positive tumours because tumours arising in such people usually harbor less LOH and a lower *TP53* mutation rate than smokers [36-38]. Contrary to our expectation, the global copy number changes at the chromosomal arm level did not differ between the two groups, although significant differences of alteration frequency at the individual chromosomal arms were seen. In addition, only *ALK* fusion-negative tumours showed an increase of the frequency of chromosome arm gain with the advancement of disease stage. Furthermore, at the smaller-genomic scale level, *ALK* fusion-positive tumours were less amplified at the loci containing *EGFR* family genes, 7p11.2 (*EGFR*), 17q12 (*ERBB2*) and other loci, 1p34.3 (*MYCL*), 7p21.1, 8q24.21 (*MYC*), 16p13.3 and 17q25.1. *EGFR* and *ERBB2* play important roles by dimerizing when their ligands binds to produce downward growth signals to the tumour cells. Mutations and activation of these genes may drive carcinogenesis [39], and increased expression is associated with a poor prognosis in NSCLCs [40-43]. *ALK* fusion positive tumours are speculated to be less dependent on the actions of oncogenes and tumour-suppressor genes induced by copy number changes. Our results may also indicate that there

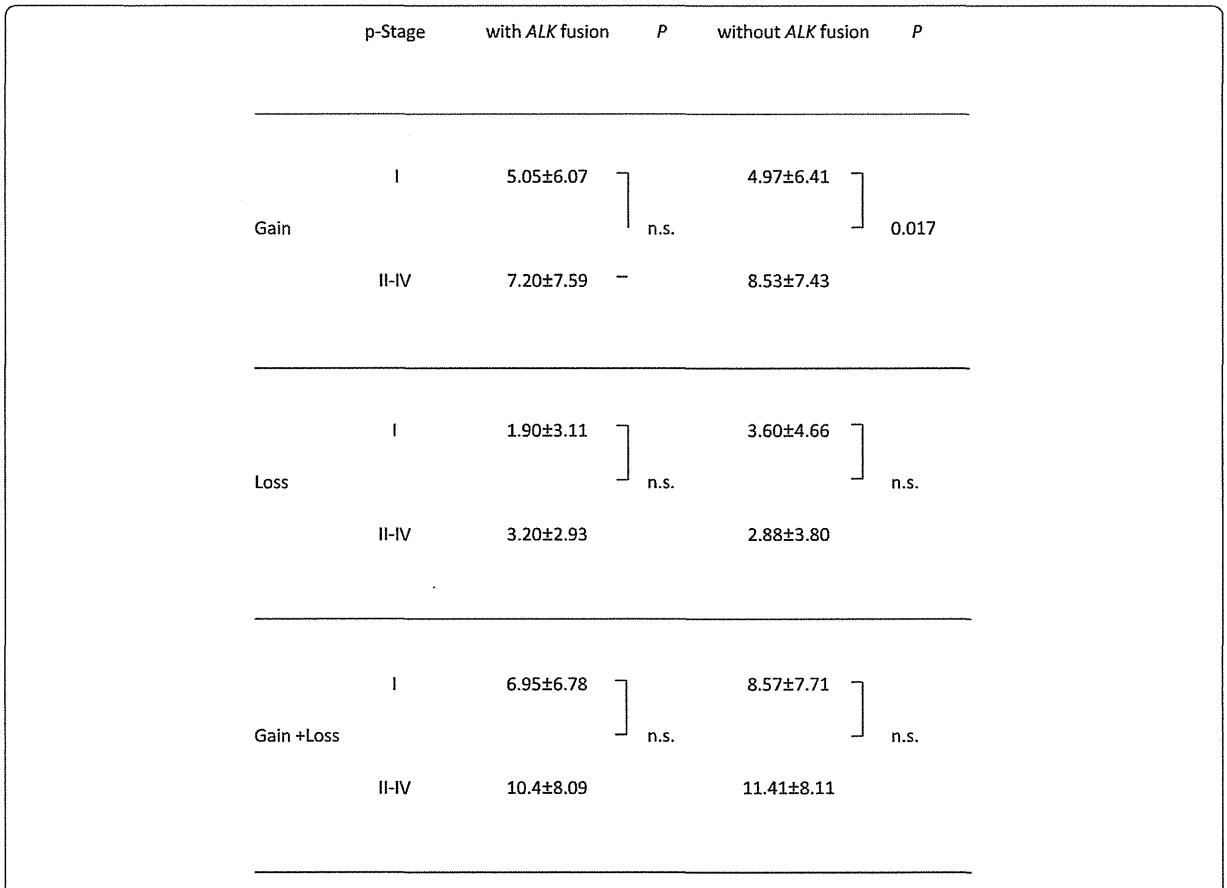

Figure 2 Comparisons of numbers of chromosome arms altered with or without *ALK* fusion in different pathological stages. Note that, whereas tumours in higher stages show more gains than stage I tumours when the tumours have no *ALK* fusion, *ALK* fusion positive tumours exhibit no such difference. p-Stage; pathological stage, n.s.; not statistically significant.

is common and frequent chromosome abnormality in lung adenocarcinomas independent of *ALK* fusion, such as the 5p15.33 region, including *TERT*.

As for genomic loss, 9p21.3 (*CDKN2A*), 9p23-p24.1 (*PTPRD*) and 13q14.2 (*RB1*) were significantly less frequently deleted in *ALK* fusion-positive tumours. Homozygous deletion was seen only at 9p21.3 including *CDKN2A* and limited to *EGFR*-mutated tumours among *ALK* fusion-negative neoplasms as reported in the literature [44] and also seen in *ALK*-fusion positive ones. That deletion of 9p23-24.1 and 13q14.2 including tumour suppressor genes was rare in *ALK* fusion-positive tumours suggests that they can grow even if the functions of these suppressor genes are retained.

Of all the selected loci, 5p15.33 containing *TERT* (telomerase reverse transcriptase isoform 2) showed the highest frequency of recurring gain regardless of *ALK* fusion. The enzyme is important for telomere regeneration and maintenance resulting in a growth advantage and Zhang et al. reported that the locus is a frequent target of amplification during tumourigenesis [45]. Copy number gain of this locus significantly correlates with telomerase activity [46] and is one of the most consistent alterations in the early stages of non-small cell lung cancer [47]. In addition, increased susceptibility to lung cancer development associated with a SNP polymorphism of this locus has been reported [48,49]. The fact that most human tumour cells have telomerase activity indicates that its acquisition is vital for carcinogenesis and cell immortalization, and it might explain the reason why lung adenocarcinomas with or without *ALK* fusion shows similar frequency of copy number gain of this locus.

Our results have some therapeutic relevance. The fact that there are less involvement of other oncogenes and tumor suppressor genes may be related to dramatic responses to targeted drugs because of intact cellular processes including apoptosis pathways. In this regard, there is an interesting paper by Camidge et al. [50], demonstrating the inverse relationship between fused and isolated red copy number on FISH might suggest

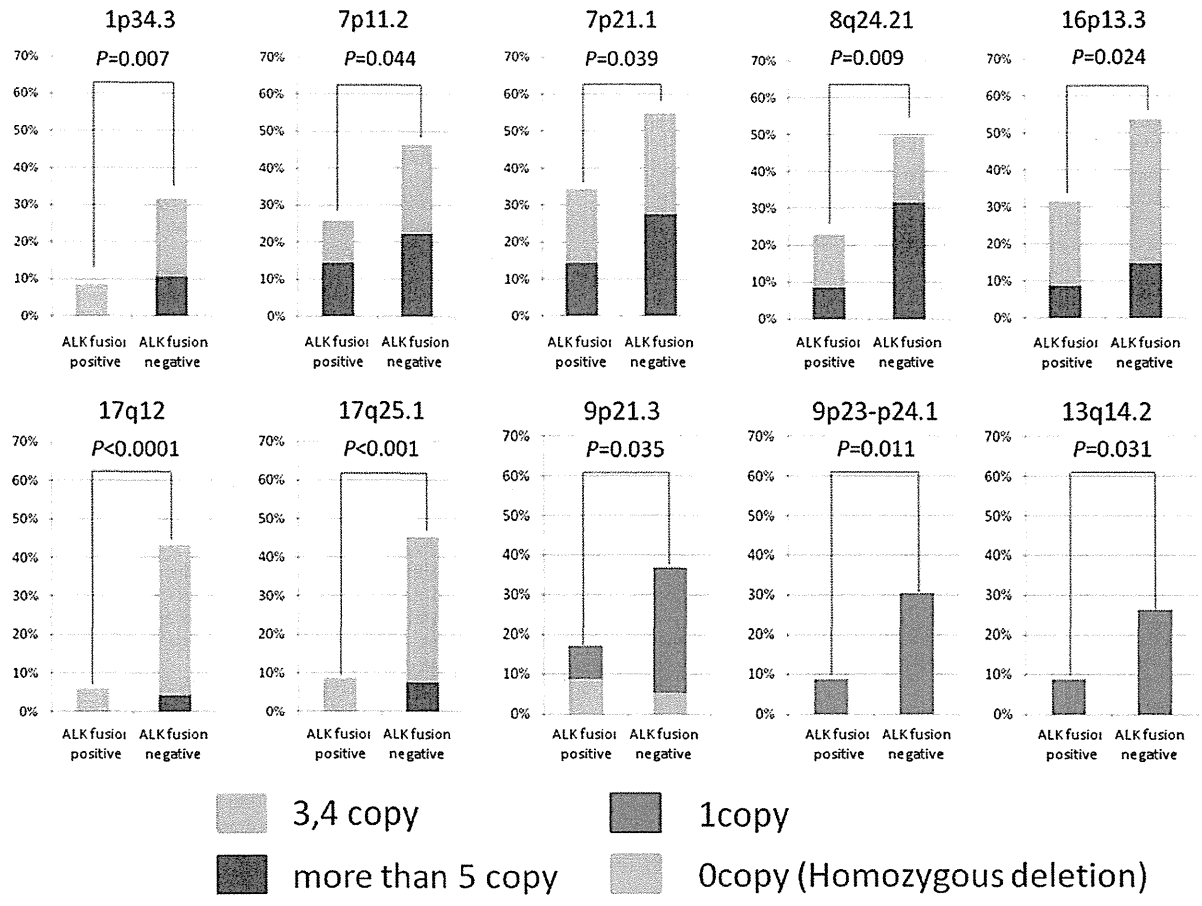

Figure 3 Significant differences in copy number change detected at seven loci for gain and three loci for loss among twenty-six selected loci. Colors of the stacked bars represent copy number: orange, 3,4 copies; red, ≥ 5 copies; blue, 1 copy loss (heterozygous deletion), light green: 2 copy losses (homozygous deletion). 17q12, 17q25.1 show remarkable differences in copy number gain between *ALK* fusion-positive and -negative tumours.

the *ALK* fusion positive tumor was a "near-diploid" subtype of non-small cell lung cancer. Comparing closely, however, between their and our results, our study clearly revealed the overall frequency of chromosome aberrations are similar between *ALK* fusion positive and negative tumors, suggesting not "near-diploid". But, certainly, we need more investigations on genomic instability of *ALK* fusion positive tumors.

It is well known that smoking causes genomic changes with allelic imbalance [20]. As shown in Table 1, smokers dominate never smokers in the group without fusion whereas the fusion-positive group has more never smokers than smokers. Since the tumors without *ALK* fusion include *EGFR*-mutated tumors, most of which are from never smokers, the *ALK* fusion-negative group is certainly heterogeneous. In due course, a study that describes comparisons of allelotypes of non-smoker's tumors between with *ALK* fusion and with *EGFR* mutation should be warranted.

Conclusions

Although overall frequencies of aberrations at the chromosome arm level do not appear to significantly differ between *ALK* fusion-positive and -negative tumors, smaller genomic regions including cancer-related genes do show significant variation. Thus tumors with *ALK* fusion feature significantly fewer copy number gains and losses at loci containing oncogenes and tumor-suppressor genes, respectively. This implies that *ALK* fusion itself exerts very strong driving forces for tumorigenesis, in other words, that *ALK* fusion is a driver mutation, not just a passenger mutation.

Additional files

Additional file 1: Table S1. Frequencies of fusion variants of *ALK* rearrangements. **Table S2.** Cases with *TP53* mutations and their smoking status. **Table S3.** Chromosomal arms and number of cases with gain with or without ALK fusion. **Table S4.** Chromosomal arms and number